ISSN 1560-8034, 1605-6582 (On-line), SPQEO, 2019. V. 22, N 4. P. 410-417.

Hetero- and low-dimensional structures

Optimization of morphology of submonolayer metallic nanoparticles to enhance light trapping on a semiconductor surface

V.Z. Lozovski[1], A. De Sio[2], C. Lienau[2], G.G. Tarasov[3], T.A. Vasyliev[1], Z.Ya. Zhuchenko[3]

[1]*Taras Shevchenko National University of Kyiv, 60, Volodymyrska, 01033 Kyiv, Ukraine*
[2]*Institut für Physik, Carl von Ossietzky Universität Oldenburg, Ammerländer Heerstraße 114-118, D-26129 Oldenburg, Germany*
[3]*V. Lashkaryov Institute of Semiconductor Physics, National Academy of Sciences of Ukraine, 45, prospect Nauky, 03680 Kyiv, Ukraine*
E-mail: tarasov@isp.kiev.ua

Abstract. The problem of light trapping engineering for semiconductor surfaces covered with randomly distributed spheroidal metallic nanoparticles has been considered. The absorption of incident light by such a structure has been calculated using the Green functions method, involving the concept of an effective susceptibility. A target function, optimizing broad-band light absorption throughout the visible range has been constructed taking the geometry of the structure as the control parameters. The optimization problem of light-trapping in such structure has been solved, and the optimum nanoparticle coverage for matching the required shape of absorption spectra has been obtained. Our results can be applied to the design of plasmonic-enhanced light-collecting elements in solar cells.

Keywords: semiconductor surface, metallic nanoparticle, effective susceptibility, optical absorption, target function.

https://doi.org/10.15407/spqeo22.04.410
PACS 42.25.Bs, 42.79.Wc, 73.20.Mf, 78.67.Bf, Qa, -n

Manuscript received 04.09.19; revised version received 24.09.19; accepted for publication 29.10.19; published online 08.11.19.

1. Introduction

The design of efficient solar cells is a crucial issue in renewable energy research. Light absorption in the active layer of the device may be restricted by the low electric field inside high-refractive index semiconductors and the small time of interaction of the incident light with the active semiconductor material. The resulting low absorption can limit the performance, especially in thin and ultrathin film solar cells [1-3]. Surface texturing is considered as an effective strategy to enhance light-collection in the active layer, in particular in thin film solar cells [3, 4]. Optimization of the texture of back-contacts, aimed at achieving longer light paths in the active layer, includes, for example, evolution-inspired strategies [5]. Another approach exploits plasmonic-enhancement, by, *e.g.*, metallic gratings or arrays of metallic nanoparticles [2]. In this case, the resonant excitation of surface plasmons at the interface between the metallic elements and semiconductor active layer leads to significant enhancement of both the strength of the electric field and light path in the active layer [6-9]. For silicon solar cells, plasmonic-enhancement of light collection has been reported for both random [10] and quasi-periodic [11] arrays of metallic nanoparticles covering the semiconductor surface. The introduction of metallic nanoparticle arrays with different morphologies at the front and rear surfaces of the active layer of thin (few micrometers) silicon solar cells has been also shown to significantly modify the transmission of light at these contacts. Specifically, optimized morphologies to increase transmission at the front contact, while reducing it at the rear one, have been intensively discussed [12].

In this paper, the authors deal with the problem of engineering light trapping in a semiconductor surface that is covered with metallic spheroidal nanoparticles randomly distributed over its surface. Crystalline silicon is taken as a prototypical model semiconductor for a crystalline solar cell material. We optimize morphology of the sub-monolayer of metallic particles on the top of a silicon slab by calculating the absorption of the mono-layer structure over the entire visible spectral range using the Green functions method by employing an effective susceptibility concept. We employ a pattern-search approach to find a solution of the optimization problem, taking the angle-of-incidence of the impinging light as

well as the shape and surface coverage of the nanoparticles as control parameters. We show that an efficient coupling of the incident light to both the transverse and longitudinal plasmon resonance of ellipsoidal nanoparticles can profoundly enhance the light trapping efficiency. This improvement in light absorption by morphology optimization is demonstrated by calculating the absorption spectra of the layered system throughout the visible and near-infrared spectral ranges.

Statement of the problem

In practically meaningful problems of light-trapping in solar cells, the absorption profile is expected to be near constant value in the visible spectral range [5, 12]. For example, in Ref. [5], 31 wavelengths evenly distributed in the visible range are considered as incident light for broadband optimization. The optimized absorption spectrum varied near some constant value and the average absorption over the whole spectrum reached 0.481. In Ref. [12], optimal light trapping was achieved in the visible range by means of homogeneous plasmonic enhancement by a submonolayer of silver nanoparticles covering the silicon surface. Thereof, it seems quite reasonable to take as a target of optimization some constant value of local field enhancing, including the absorption in the system of nanoparticles. Similarly, the difference between the maximum and minimum values of the absorption in theoretical studies is taken to be no more than a factor of ten [13]. We try to meet these requirements using a hybrid metal nanoparticle/semiconductor structure with a geometry that is shown in Fig. 1. We consider a slab of silicon with a thickness of few micrometers and dielectric permittivity ε_m, which is covered with a submonolayer of randomly arranged spheroidal metallic nanoparticles of the volume V_p. We consider gold, copper and silver nanoparticles with dielectric permittivities obtained by interpolation of the experimental data reported in Ref. [14]. We denote via z_p the distance between the center of particles and semiconductor surface. The axis z is perpendicular to the semiconductor surface defined as the x-y plane. The parameter $\kappa = a_z/a_x$ characterizes the shape of the particles. The light, with electric field vector $\vec{E}$, propagates along the direction $\vec{k}$, entering the system of nanoparticles and silicon thin film at the angle of incidence θ (Fig. 1).

Light absorption by the system of nanoparticles at the frequency ω is proportional to the ratio of the dissipative function $Q\left(\vec{k}_\parallel, z_p, \omega\right)$ and the energy density of the external electromagnetic field $\vec{E}^0\left(\vec{k}, z_p, \omega\right)$ [15]:

$$I\left(\vec{k}_\parallel, r_p, \omega\right): \frac{Q\left(\vec{k}_\parallel, r_p, \omega\right)}{\left|\vec{E}^0\left(\vec{k}_\parallel, r_p, \omega\right)\right|^2}. \qquad (1)$$

Here, the Cartesian components of the electric field are denoted as $l = x, y, z$ and a summation convention is used. $\vec{k}_\parallel$ is the in-plane component of vector $\vec{k}$.

Eq. (1) gives the total absorption spectrum of the layered hybrid structure. The dissipative function can be defined through the local field $\vec{E}\left(\vec{k}_\parallel, z_p, \omega\right)$ and the local current $\vec{J}\left(\vec{k}_\parallel, z_p, \omega\right)$,

$$Q\left(\vec{k}_\parallel, z_p, \omega\right) = n\,\mathrm{Re}\left[\vec{E}^*\left(\vec{k}_\parallel, z_p, \omega\right)\cdot \vec{J}\left(\vec{k}_\parallel, z_p, \omega\right)\right], \qquad (2)$$

where $n = N\pi r_p^2$, while N is the number of particles per unit of surface, and n is the fraction of the surface area covered with nanoparticles. The relations between fields and local currents were obtained in the framework of the Green functions method by using the effective susceptibility concept [16] as

$$J_i\left(\vec{k}_\parallel, z_p, \omega\right) = -i\omega X_{ij}\left(\vec{k}_\parallel, z_p, \omega\right) E_j^{(0)}\left(\vec{k}_\parallel, z_p, \omega\right) \qquad (3)$$

and

$$E_i\left(\vec{k}_\parallel, z_p, \omega\right) = \left(\chi_{ji}^{(p)}(\omega)\right)^{-1} \mathrm{X}_{jl}\left(\vec{k}_\parallel, z_p, \omega\right) E_l^{(0)}\left(\vec{k}_\parallel, z_p, \omega\right). \qquad (4)$$

In a general case, the local field $\vec{E}\left(\vec{R}, \omega\right)$ in the system of nanoparticles is described by means of the self-consistent equation [16]

$$E_i\left(\vec{R}, \omega\right) = E_i^{(0)}\left(\vec{R}, \omega\right) - \\ - k_0^2 \sum_p \int_{V_p} G_{il}^{1,1}\left(\vec{R}, \vec{R}', \omega\right) \chi_{lj}^p(\omega) E_j\left(\vec{R}', \omega\right) d\vec{R}'. \qquad (5)$$

Here, $\vec{R}$ is a radius-vector, $k_0 = \omega/c$, $G_{il}^{1,1}\left(\vec{R}, \vec{R}', \omega\right)$ – Green's dyadic with source and observation points in upper half-space [17, 18]. Summation in the left side of (5) was performed over all nanoparticles with spatial locations $\vec{R}'$. According to Refs. [19] and [15], averaging the self-consistent equation (5) over the nanoparticle location on the surface of semiconductor, one can derive relation (4) with assumption that the sizes of nanoparticles are much smaller than the wavelength of incident light. In this case, the effective susceptibility $X_{ij}\left(\vec{k}_\parallel, z_p, \omega\right)$ of a submonolayer of particles takes the following form:

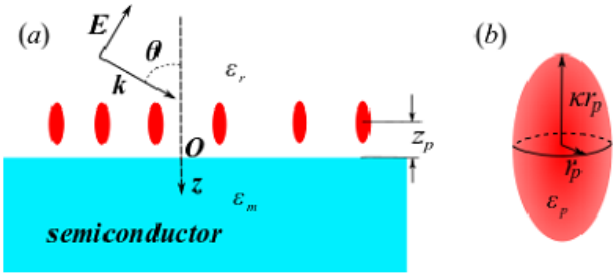

Fig. 1. Sketch of the considered system: (a) semiconductor covered with identical metallic nanoparticle spheroids (b) with rotation axis directed along z (semi-axes $a_x = a_y = r_p$).

$$X_{ij}\left(\vec{k}_{\parallel},z_p,\omega\right)=\left[\left(\chi_{ij}^{(p)}(\omega)\right)^{-1}+nk_0^2G_{ji}^{1,1}\left(\vec{k}_{\parallel},z_p,\omega\right)\right]^{-1}, \quad (6)$$

where $G_{ji}^{1,1}\left(\vec{k}_{\parallel},z_p,\omega\right)$ is the Fourier transform of Green's dyadic. We denote with $\chi_{ij}^{(p)}(\omega)$ the susceptibility of a single spheroidal nanoparticle at the surface [20]:

$$\chi_{ij}^{(p)}=\begin{pmatrix}\chi_{\parallel}(\omega) & 0 & 0\\ 0 & \chi_{\parallel}(\omega) & 0\\ 0 & 0 & \chi_{\perp}(\omega)\end{pmatrix},$$

$$\chi_{\parallel,\perp}=\varepsilon_r V_p\frac{\varepsilon_p(\omega)-\varepsilon_r}{\varepsilon_r+\left(\varepsilon_p(\omega)-\varepsilon_r\right)m_{\parallel,\perp}}L_{\parallel,\perp}, \quad (7)$$

where ε_r is the dielectric permittivity of the environment in the upper half-space, $\varepsilon_p(\omega)$ – dielectric permittivity function of the nanoparticles. The shape factor of the particles

$$L_{\parallel,\perp}=\left[1+\frac{\left(\varepsilon_r-\varepsilon_m\right)\left(\varepsilon_p(\omega)-\varepsilon_r\right)}{3\left(\varepsilon_r+\varepsilon_m\right)\left(\varepsilon_r+\left(\varepsilon_p(\omega)-\varepsilon_r\right)m_{\parallel,\perp}\right)}\mathrm{U}_{\parallel,\perp}\right] \quad (8)$$

is presented via the depolarization factor $m_{\parallel,\perp}$ that has the form

$$m_{\perp}=\frac{\zeta}{(1-\zeta)^{3/2}}\left(\frac{1}{2}\ln\frac{1+\sqrt{1-\zeta}}{1-\sqrt{1-\zeta}}-\sqrt{1-\zeta}\right),$$

$$m_{\parallel}=0.5\left(1-m_{\perp}\right),\ \zeta=\kappa^{-2}, \quad (9a)$$

for prolate spheroids, $\kappa>1$, and

$$m_{\perp}=\frac{\zeta}{(\zeta-1)^{3/2}}\left(\sqrt{\zeta-1}-\mathrm{arcth}\sqrt{\zeta-1}\right),$$

$$m_{\parallel}=0.5\left(1-m_{\perp}\right) \quad (9b)$$

for oblate spheroids, $\kappa<1$.

In Eq. (8), $\mathrm{U}_{\parallel}=a_xa_ya_z/\left(2z_p\right)^3=\kappa\left(r_p/2z_p\right)^3$, $\mathrm{U}_{\perp}=2\mathrm{U}_{\parallel}$. For further details, see Ref. [20]. Here, we consider the special case of elliptical particles with $a_x = a_y$. These elliptical particles have interesting spectroscopic properties [21]. In addition to a transverse surface plasmon (SP) resonance, similar to the SP resonance of a small spherical particle and excited with light that is polarized along the short axis of the ellipsoid, their optical spectra show a distinct longitudinal SP resonance, excited with light polarized along the long axis of the particle. This longitudinal SP resonance undergoes a distinct red shift with increasing ellipticity $\kappa=a_z/a_x$. Incident light with a polarization state that is chosen to couple to both SP resonances can therefore be absorbed in a very broad spectral range from the UV part to the near-infrared one. Therefore, coverage of the semiconductor surfaces with these elliptical nanoparticles gives a particularly large flexibility in tailoring the optical absorption of the hybrid structure. We analyze absorption only in particles, but not in silicon, because we are primarily interested in the plasmonic resonance of coverage, which can be fixed with the help of dissipative function (2). In the experimental work [22], it was shown that the solar cell coverage with gold nanoparticles of 50-, 80-, 100-nm diameters increased the photocurrent for the entire visible range of light. The maximum increase of efficiency was observed near plasmonic resonance. This is the motivation for choosing such a coverage in our work. We also note that we consider only prolate particles with comparatively small radii $a_x = a_y = r_p$ of 10 nm. For such small particles, the quasi-static model for the susceptibility outlined above is valid and the shape of the spectra is basically independent of the value of the nanospheroid short axis. For larger particle radii, the effects of finite retardation are needed to be considered but this is beyond the scope of the present work.

We now turn to the optimization problem aimed at designing a user-defined shape of the absorption spectrum of the hybrid structure as given by Eq. (1). For this purpose, we construct the target function $Tf\left(\kappa,f_p,\theta\right)$:

$$Tf\left(\kappa,f_p,\theta\right)=\frac{1}{N_1}\sum_{1.65\mathrm{eV}<\hbar\omega<3.25\mathrm{eV}}\left[I\left(\vec{k}_{\parallel},z_p,\omega\right)-I_0(\omega)\right]^2, \quad (10)$$

where $I_0(\omega)$ is the desired absorption profile, and N_1 – number of colors at which the simulated spectrum is compared to the desired spectrum, *i.e.*, the number of terms in the sum (10).

The aim of optimization problem is to find the values of κ,f_p,θ for which

$$Tf\left(\kappa,f_p,\vartheta\right)\to\min. \quad (11)$$

Here, κ is the shape parameter defining the ellipticity of the particles, θ – angle of incidence of the optical field impinging on the system, and f_p is the surface coverage by the nanoparticles. The value of f_p is restricted within the interval $0\le f_p\le f_p^{\max}$. This restriction arises because of the average distance between nanoparticles should be no shorter than the diameter of nanoparticles in the plane of the silicon surface [2]. Therefore, the maximum concentration of nanoparticles $f_p^{\max}-0.2$ is used in the present model, and we also consider an effective target function

$$Tf_{eff}\left(\kappa,f_p,\vartheta\right)=$$

$$=Tf\left(\kappa,f_p,\vartheta\right)+\alpha_1\left[f_p-f_p^{\max}\right]^{+}+\alpha_2\left[-f_p\right]^{+}, \quad (12)$$

where α_1 and α_2 are positive constants chosen from the theory of constrained optimization and the Karush–Kuhn–Tucker (KKT) conditions [23]: $[a]^{+}=\mathrm{Max}\{0,a\}$.

Taking the additional restriction of the surface coverage into account, the unconstrained problem (11) can be represented as the minimum of the effective target function (12). The second and the third terms in the right-hand side of (12) with α_1 and α_2 are non-zero, when the surface density falls out of the restrictions $0 \le f_p \le f_p^{\max}$.

2. Results and discussion

In what follows, we consider the simplest conceivable absorption profile, *i.e.*, $I_0(\omega) = I_0$= const, as a target spectrum for the hybrid layer illuminated with *p*-polarized light. To perform the optimization of the target function (11) or (12), we use the pattern search method [23]. In order to get a first approximation, one can plot contour maps of the distribution of target function values as a function of the shape parameter κ and the angle of incidence θ at fixed surface coverage with nanoparticles of 0.1 (Fig. 2).

The contour maps show black circles marking the region with the smallest values of the target function. Taken the position of the center of dark spots with the surface density as the first approach for the pattern search, one can obtain the optimized configuration by further optimization of all three control parameters. In all cases, less than 20 cycles of pattern search are necessary for the optimization problem to converge with an error of 10^{-3}.

The dependence of the optimized parameters on the number of nodes *N* in (11) or (12) for different nanoparticle materials and substrates is shown in Tables 1 and 2. In all the cases, with increasing the number of nodes, the minimum value of the target function (11) decreased. The optimized values of the shape parameter κ and the angle of incidence θ are asymptotically approximated by some fixed values. The optimized surface coverage in the case of gold and silver nanoparticles reaches a predefined limiting value of 0.2. This means that the target function (12) was optimized. By contrast, for copper particles, it suffices to optimize the target function (11). Specifically, for copper nanoparticles, the optimized configuration results in the smallest target function $Tf_{\min} \approx 0.00446$ with $\kappa_{opt} \approx 5.48$, $f_{opt} \approx 0.094$, and $\theta_{opt} \approx 0.487$ or $\theta_{opt} \approx 28°$ for 101-points approximation. Similarly, for gold nanoparticles, the configuration of the smallest target function $Tf_{\min} \approx 0.0147$ is $\kappa_{opt} \approx 5.334$, $f_{opt} \approx 0.2$ and $\theta_{opt} \approx 0.295$ or $\theta_{opt} \approx 16.9°$ for 101-points approximation. The optimized values of absorption for gold and copper nanoparticles arrays are close to the target value of $I_0 = 0.5$. For silver nanoparticles, however, the effective absorption is much lower, most likely since interband absorption effects are considerably reduced as compared to those in gold and copper. We have therefore limited the target value to $I_0 = 0.2$.

Comparison of the data of Tables 1 ($\varepsilon_s = 4$) and 2 ($\varepsilon_s = 12$) shows that the optimized surface density of nanoparticles weakly depends on the dielectric function of substrate ε_s. This can be nicely seen for, *e.g.*, gold nanoparticles in Fig. 3a, where a smooth increase of the optimized shape parameter κ_{opt} with the increasing ε_s can be observed. Similarly, a smooth dependence of the

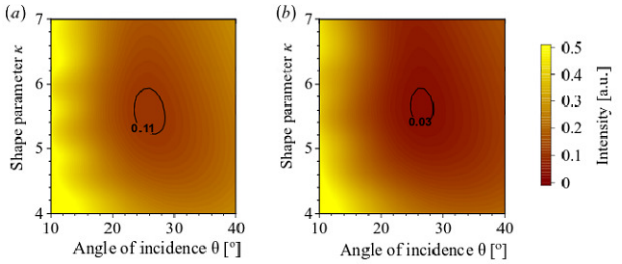

Fig. 2. Contour maps of the target function for surface coverage with 0.1 density for (a) gold and (b) copper nanoparticles with rotation axis directed along OZ ($a_x = a_y$), $\varepsilon_s = 4$, *p*-polarized light.

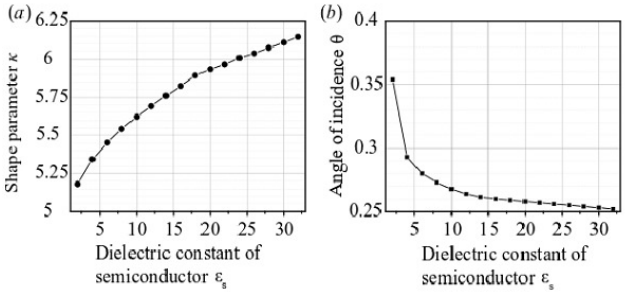

Fig. 3. (a) Dependence of the optimized shape of gold nanoparticles and (b) that of the angle of incidence of external light on the dielectric function of the semiconductor substrate for *p*-polarized external light.

optimized values of angles of incidence on ε_s is seen in Fig. 3b. By means of the data in Tables 1 and 2 as well as the curves in Fig. 3, one can theoretically predict the optimized morphologies of gold nanoparticle arrays on a semiconductor surface for a wide range of dielectric function values ε_s.

We calculated the absorption spectra (Fig. 4) for optimized configurations of a semiconductor layer with $\varepsilon_s = 4$ covered with (a) copper and (b) gold nanoparticles. We found that the optimized nanoparticles (Table 1) significantly increase the absorption at all wavelengths in the visible spectral range (Fig. 4, top curves (red)). As seen in Table 1, an increase in the number of spectral nodes in the target function (11) or (12) results in a slightly improved match of the target spectrum (Fig. 4, straight lines (black)). Similarly, also the optimized configurations for a larger dielectric function of the substrate (Table 2) significantly increase the absorption at all wavelengths in the visible range, as shown in Fig. 5. Importantly, in stark contrast to the absorption spectra of spherical particles (bottom lines (blue) in Figs. 4 and 5), the optimized absorption spectrum not only shows a significant absorption for the wavelengths below 600 nm. All optimized spectra display a distinct long wavelength absorption band around 700 nm, resulting from the coupling of the external light to the longitudinal SP resonance of the elliptical nanoparticles. Evidently, the ability to couple light to both the transverse and longitudinal SP resonances of the elliptical nanoparticle dramatically enhances the absorption throughout the visible and near-infrared spectral ranges.

Table 1. Optimized values of the target function and parameters κ, f_p, θ, $\varepsilon_s = 4$, *p*-polarized external light.

N		$Tf_{\min}$	κ_{opt}	f_{opt}	θ_{opt}	I_0
Cu	6	0.00446	5.914	0.094	0.468	0.5
	11	0.00461	5.672	0.092	0.487	0.5
	21	0.00446	5.566	0.093	0.488	0.5
	51	0.00427	5.502	0.094	0.487	0.5
	101	0.00419	5.480	0.094	0.487	0.5
Au	6	0.0157	5.775	0.2	0.278	0.5
	11	0.0160	5.564	0.2	0.293	0.5
	21	0.0152	5.444	0.2	0.294	0.5
	51	0.0148	5.369	0.2	0.295	0.5
	101	0.0147	5.344	0.2	0.295	0.5
Ag	6	0.0142	7.030	0.2	0.200	0.2
	11	0.0137	6.799	0.2	0.237	0.2
	21	0.0128	6.465	0.2	0.259	0.2
	51	0.0127	6.498	0.2	0.275	0.2
	101	0.0126	6.455	0.2	0.280	0.2

Table 2. Optimized values of the target function and parameters κ, f_p, θ, $\varepsilon_s = 12$, *p*-polarized external light.

N		$Tf_{\min}$	κ_{opt}	f_{opt}	θ_{opt}	I_0
Cu	6	0.00619	6.098	0.092	0.418	0.5
	11	0.00652	5.862	0.088	0.442	0.5
	21	0.00648	5.743	0.089	0.440	0.5
	51	0.00630	5.673	0.090	0.440	0.5
	101	0.00623	5.650	0.090	0.441	0.5
Au	6	0.0174	6.041	0.2	0.258	0.5
	11	0.0170	5.911	0.2	0.264	0.5
	21	0.0165	5.739	0.2	0.263	0.5
	51	0.0165	5.642	0.2	0.262	0.5
	101	0.0164	5.610	0.2	0.262	0.5
Ag	6	0.0123	7.295	0.2	0.215	0.2
	11	0.0124	7.114	0.2	0.242	0.2
	21	0.0115	7.053	0.2	0.266	0.2
	51	0.0114	6.956	0.2	0.284	0.2
	101	0.0112	6.935	0.2	0.291	0.2

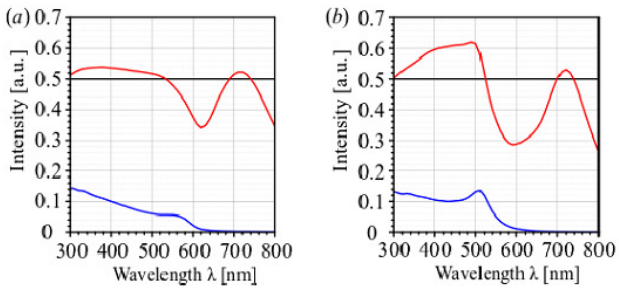

Fig. 4. The absorption spectra for (a) copper nanoparticles and (b) gold nanoparticles. The bottom curves (blue) correspond to the absorption spectra of a sufficiently low density of spherical nanoparticles. The straight lines (black) show the target spectra. The top curves (red) correspond to optimized configurations of nanoparticles coverages, $\varepsilon_s = 4$, *p*-polarized external light (Color online).

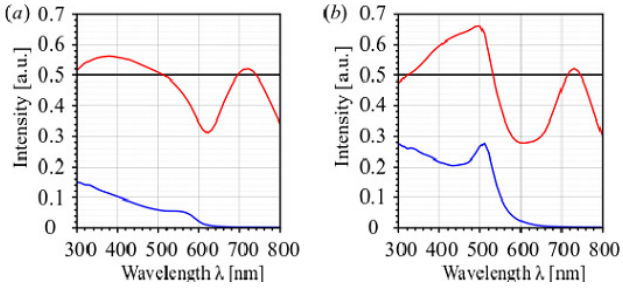

Fig. 5. The absorption spectra for (a) copper nanoparticles and (b) gold nanoparticles. The bottom curves (blue) correspond to the absorption spectra of a sufficiently low density of spherical nanoparticles. The straight lines (black) show the target spectra. The top curves (red) correspond to optimized configurations of nanoparticles coverages, $\varepsilon_s = 12$, *p*-polarized external light (Color online).

Our analysis of optimization shows that coverages consisting of the needle-like nanoparticles with the length near 110…140 nm provide efficient absorption in all the visible range. Nanoparticles are big enough and absorption in them is much less than the scattering by them into the semiconductor substrate. In the work [7], it was shown that, for spherical nanoparticles with the diameter larger than 60 nm, the effective scattering area is much larger than the effective absorption area. Although the effective values of scattering and absorption have to be taken into account for further studies, the shape of our optimized nanoparticles is in well qualitative accordance with the results of scattering by oblate and prolate single spheroidal nanoparticles on semiconductor surface [20] and with the results of optimization of coverage inherent to the silicon surface with an oblate cylinder or hemisphere [2].

The optimized spectra in Figs. 4a, 5a and Figs. 4b, 4b are qualitatively similar, showing a comparatively moderate influence of the substrate on the optimized absorption spectrum. Using the optimized shape parameters and angles of incidence of the light field from Fig. 3, one can, in this manner, calculate the absorption spectra of metallic nanoparticle arrays for a broad range of dielectric functions ε_s and, hence, for several different types of semiconductor substrates.

3. Conclusions

In conclusion, we have shown a theoretical approach to optimization of plasmonic-enhanced absorption by metallic nanoparticle arrays on the surface of a semiconductor. In our work, we have considered elliptical nanorods with short-axis diameters of 20 nm. The absorption of light for different semiconductor substrates covered with sub-monolayer of metallic spheroidal nanoparticles has been calculated in the framework of the effective susceptibility concept [16, 19]. Taking a spectrally flat absorption spectrum throughout the visible and near-infrared spectral ranges as a target, we have optimized the optical properties of our sample by varying the shape and surface coverage of the nanoparticles as well as the angle of incidence of the external *p*-polarized light. We have shown that an optimized coupling to both the transverse and longitudinal plasmon resonance of suitably shaped elliptical particles can drastically enhance the absorption throughout the entire spectral range, resulting in a substantial improvement in light trapping efficiency over that reached for spherical nanoparticles. Our results suggest that engineering morphology of metallic nanoparticle arrays by controlling the particle density and shape significantly enhances light absorption over a broad spectral range. In the present study, we have focused on optimization of the absorption spectrum, resulting both in an enhancement of the desired absorption within the semiconductor but also to a substantial increase in the amount of light that is absorbed by the metal nanoparticles. Since this light is partially transferred into heat due to the unavoidable Ohmic damping of the surface plasmon mode, it does only partially contribute to an enhanced light trapping by the semiconductor substrate. In the future work, we aim at using similar strategies to directly optimize the power conversion efficiency of solar cell devices covered with metallic nanostructures by implementing more realistic models for the current transport through the device. We anticipate that the optimization method developed in this work will contribute significantly to an improved light-to-current conversion efficiency of plasmonically-enhanced photovoltaic devices.

Acknowledgement

C. Lienau acknowledges financial support by the Deutsche Forschungsgemeinschaft (SPP 1839 and SPP 1840).

References

1. Catchpole K. and Polman A. Design principles for particle plasmon enhanced solar cells. *Appl. Phys. Lett*. 2008. **93**, No 19. P. 191113. https://doi.org/10.1063/1.3021072.
2. Atwater H.A. and Polman A. Plasmonics for improved photovoltaic devices. *Nature Materials*. 2010. **9**, No 3. P. 205–213. https://doi.org/10.1038/nmat2629.
3. Battaglia C., Hsu C.-M., Söderström K. *et al*. Light trapping in solar cells: Can periodic beat random? *ACS Nano*. 2012. **6**, No 3. P. 2790–2797. https://doi.org/10.1021/nn300287j.
4. Campbell P. and Green M.A. Light trapping properties of pyramidally textured surfaces. *J. Appl. Phys.* 1987. **62**. P. 243. https://doi.org/10.1063/1.339189.
5. Wang C., Yu S., Chen W., and Sun C. Highly efficient light-trapping structure design inspired by natural evolution. *Sci. Rep*. 2013. **3**. P. 1025. https://doi.org/10.1038/srep01025.
6. Catchpole K.R. and Pillai S. Absorption enhancement due to scattering by dipoles into silicon waveguides. *J. Appl. Phys.* 2006. **100**. P. 044504. https://doi.org/10.1063/1.2226334.
7. Pillai S., Catchpole K.R., Trupke T., and Green M.A. Surface plasmon enhanced silicon solar cells. *J. Appl. Phys.* 2007. **101**. P. 093105. https://doi.org/10.1063/1.2734885.
8. Ferry V.E., Sweatlock L.A., Pacifici D., and Atwater H.A. Plasmonic nanostructure design for efficient light coupling into solar cells. *Nano Lett*. 2008. **8**, No 12. P. 4391–4397. https://doi.org/10.1021/nl8022548.
9. Wang W., Wu S., Reinhardt K., Lu Y., and Chen S. Broadband light absorption enhancement in thin-film silicon solar cells. *Nano Lett*. 2010. **10**, No 6. P. 2012–2018. https://doi.org/10.1021/nl904057p.
10. Nakayama K. Tanabe K., and Atwater H.A. Plasmonic nanoparticle enhanced light absorption in GaAs solar cells. *Appl. Phys. Lett*. 2008. **93**. P. 121904. https://doi.org/10.1063/1.2988288.

11. Mokkapati S., Beck F.J., Polman A., and Catchpole K.R. Designing periodic arrays of metal nanoparticles for light-trapping applications in solar cells. *Appl. Phys. Lett.* 2009. **95**, 053115. https://doi.org/10.1063/1.3200948.
12. Sun C. and Wang X.Q. Efficient light trapping structures of thin film silicon solar cells based on silver nanoparticle arrays. *Plasmonics*. 2015. **10**, No 6. P. 1307–1314. https://doi.org/10.1007/s11468-015-9934-1.
13. Hajimirza Sh., Howell J.R. Robust nanoscale patterns for thin film solar cells using inverse optimization of nonuniformly sampled absorption spectrum. *Proc. ASME 2011 International Mechanical Engineering Congress & Exposition*, IMECE2011, November 11-17, 2011, Denver, Colorado, USA, IMECE2011-62803.
14. Johnson P.B. and Christy R.W. Optical constants of the noble metals. *Phys. Rev. B*. 1972. **6**. P. 4370. https://doi.org/10.1103/PhysRevB.6.4370.
15. Lozovski V.Z., Lienau C., Tarasov G.G., Vasyliev T.A., Zhuchenko Z.Ya. Configurational resonances in absorption of metal nanoparticles seeded onto a semiconductor surface. *Results in Physics*. 2019. **12**. P. 1197–1201. https://doi.org/10.1016/j.rinp.2018.12.091.
16. Lozovski V., Vasilenko V., Tarasov G.G., Lienau C., Mazur Yu.I., and Salamo G.J. Dynamic configurational resonances caused by optical nonlinearities in ultra-fast near-field microscopy. *J. Opt.* 2013. **15**. P. 035204 (13 p.). https://doi.org/10.1088/2040-8978/15/3/035204.
17. Mills D.L. and Maradudin A.A. Surface roughness and the optical properties of a semi-infinite material; the effect of a dielectric overlayer. *Phys. Rev. B*. 1975. **12**. P. 2943. https://doi.org/10.1103/PhysRevB.12.2943.
18. Bah M.L., Akjouj A., Dobrzynski L. Response functions in layered dielectric media. *Surf. Sci. Rept*. 1992. **16**. 97–131. https://doi.org/10.1016/0167-5729(92)90010-9.
19. Lozovski V.Z. The effective susceptibility concept in the electrodynamics of nano-systems. *J. Computation. and Theor. Nanosci.* 2010. **7**, No 10. P. 2077–2093. https://doi.org/10.1166/jctn.2010.1588.
20. Evlyukhin A.B. and Bozhevolnyi S.I. Surface plasmon polariton scattering by small ellipsoid particles. *Surf. Sci*. 2005. **590**. P. 173–180. https://doi.org/10.1016/j.susc.2005.06.010.
21. Sönnichsen C., Franzl T., Wilk T. *et al*. Drastic reduction of plasmon damping in gold nanorods. *Phys. Rev. Lett*. 2002. **88**. P. 077402. https://doi.org/10.1103/PhysRevLett.88.077402.
22. Schaadt D.M., Feng B., and Yu E.T. Enhanced semiconductor optical absorption via surface plasmon excitation in metal nanoparticles. *Appl. Phys. Lett*. 2005. **86**. P. 063106. https://doi.org/10.1063/1.1855423.
23. Boyd S. and Vandenberghe L. *Convex Optimization*. Cambridge University Press, 2004.

Authors and CV

Valeri Lozovski,
Professor of the Institute of High Technologies, Taras Shevchenko National University of Kyiv. The scientific activities are in the theory of near-field optics and optical properties of nanocomposites.

Dr. Christoph Lienau,
Professor of Experimental Physics, Institute of Physics, University of Oldenburg, Germany. His PhD thesis was defended in 1992 at the University of Göttingen. In 2003 Habilitation in "Experimental Physics" with a thesis entitled "Optical near-field spectroscopy of semiconductor nanostructures" at the Humboldt University, Berlin. Since 2006, Full professor in physics at Carl von Ossietzky University, Oldenburg. Research interests include the questions related to probe the motion of charges, spins and nuclei in solid state and biological nanostructures on ultra-small length and ultrashort time scales. In-depth knowledge about such motions is necessary to decipher the interplay between structure and function of technologically and biologically relevant nanostructures. To gain such knowledge, his group developes, implements and applies spectroscoscopic techniques providing nanometer spatial and atto- to femtosecond temporal resolution.

Dr. Antonietta De Sio is Senior researcher in the group of Prof. Ch. Lienau at University of Oldenburg, Germany. She received the Laurea degree in 2008 from the University of Salerno, Italy and the PhD in 2012 from the University of Oldenburg, Germany. Her current research interests include the role of coupled electron and nuclear motion for the ultrafast energy and charge transport dynamics in organic functional materials and semiconducting perovskites.

Zoryana Y. Zhuchenko is Senior researcher at the V. Lashkaryov Institute of Semiconductor Physics, NASU. She graduated from Drohobych Ivan Franko State Pedagogical University in 1992 with Diploma Cum Laude in Physics and Mathematics. Since 1999 she works at the V. Lashkaryov Institute of Semiconductor Physics. In 2000, she has defended PhD Dissertation in this Institute. The main directions of her investigations are physical processes in coupled nanoscale structures of different dimensionality, in part manybody excitonic effects.

Georgiy G. Tarasov defended his candidate thesis in 1979 at the Institute of Semiconductors, Kiev, Ukraine with topic "Theory of non-linear optical effects in impure cubic crystals", and then his Doctor of Sciences thesis in 1989 under the title "Non-linear polarization spectroscopy of impure cubic crystals". Since 1997, Georgiy Tarasov is Professor in Physics of Semiconductors and Insulating Crystals at ISP NAS of Ukraine. Current research interest is physics of low-dimensional structures (quantum wells, dots, and wires), spin-doped multinary compounds and heterostructures, non-linear and linear optical properties of doped crystals and glasses.

Taras A. Vasyliev. Assistant professor of Taras Shevchenko National University of Kyiv. The area of his scientific interests includes optics of nanocomposites, submono-layer covering the semiconductor surfaces as well as mechanics of nanocomposite structures.